Impact of hydrogen energy storage on California electric power system: Towards 100% renewable electricity

Paolo Colbertaldo[a,b,], Stacey Britni Agustin[b], Stefano Campanari[a], Jack Brouwer[b]*

[a] Department of Energy, Politecnico di Milano - Via Lambruschini 4A, 20156 Milan, Italy

[b] National Fuel Cell Research Center, University of California, Irvine - Engineering Laboratory Facility, Irvine, CA, 92697-3550, United States

Abstract

Decarbonization of the power sector is a key step towards greenhouse gas emissions reduction. Due to the intermittent nature of major renewable sources like wind and solar, storage technologies will be critical in the future power grid to accommodate fluctuating generation. The storage systems will need to decouple supply and demand by shifting electrical energy on many different time scales (hourly, daily, and seasonally). Power-to-Gas can contribute on all of these time scales by producing hydrogen via electrolysis during times of excess electrical generation, and generating power with high-efficiency systems like fuel cells when wind and solar are not sufficiently available. Despite lower immediate round-trip efficiency compared to most battery storage systems, the combination of devices used in Power-to-Gas allows independent scaling of power and energy capacities to enable massive and long duration storage. This study develops and applies a model to simulate the power system balance at very high penetration of renewables. The study assesses hydrogen as the primary storage means for balancing energy supply and demand on a large scale: the California power system is analyzed to estimate the needs for electrolyzer and fuel cell systems in 100% renewable scenarios driven by large additions of wind and solar capacities. Results show that the transition requires a massive increase in both generation and storage technology, e.g., a combination of 94 GW of solar PV, 40 GW of wind, and 77 GW of electrolysis systems. A mix of technologies appears to reduce the total installation capacities required with respect to wind-dominated or PV-dominated cases. Hydrogen energy storage capacity needs are also assessed and possible alternatives are discussed, including a comparison with battery storage systems.

Keywords

Decarbonization; clean power system; 100% renewable; hydrogen energy storage; Power-to-Gas.

Highlights

- A model simulates the hourly balance of demand and supply in the power grid
- The role of storage is evaluated, focusing on hydrogen storage via Power-to-Gas
- Options for 100% renewable electricity in California are analyzed
- Constraints on operation of electrolyzer and fuel cell systems are discussed
- Needs and possibilities for hydrogen energy storage are discussed

Introduction

Attention to climate change and sustainability has increased in recent years, and these topics are now widely researched and discussed. Driven by the concern for environment and human health, international agencies and organizations call for urgent actions from all actors: research entities, governments, citizens, and industry [1,2]. All sectors involved in energy conversion, storage, or end-uses of any form are called to a transition towards low-carbon and sustainable solutions that can preserve resources and avoid ecosystem damage. Decarbonization by shifting to renewable energy sources (RES) plays a key role in the transition. Indeed, fossil fuel use not only affects natural and urban environments, but also is limited by resource availability. Although the temporal scale is not clearly defined, a switch away from fossil fuels will be unavoidable in the long term –

either caused by inadequate supply or by excessive pricing. On the contrary, renewable resources are by definition unlimited. However, they are mostly intermittent and fluctuating. To overcome their uneven distribution and dynamic availability, increased storage resources and cooperation among regions will help manage local excess renewable power generation and supply shortages.

Looking at the power sector, the system evolution to fully renewable generation is not trivial: intermittency and unbalancing affect grid behavior and energy price dynamics. Many technologies and solutions are likely to be part of the future system. Consumers will play a more active role, e.g., through demand side management [3], but increased complexity of system operation and social acceptance issues may arise. Large installed renewable capacity will produce short periods of very high priced peak generation, and substantial amounts of energy storage capacity will be needed to avoid significant electricity curtailment and manage demand-supply mismatches that occur over seconds, minutes, hours, days, and seasons. The magnitude of the challenge is big: California alone consumes 230 TWh of electricity per year, with a 50 GW peak load (2017 data [4]), currently managed mostly with fast-ramping natural gas-fired power plants.

This work investigates Power-to-Gas (P2G) as a grid-scale storage technology option for California to complement a massive increase of wind and solar installed capacity. Indeed, the full development of a hydrogen economy seems a promising way to comply with a 100% renewable electric grid requirement as envisioned by many (e.g., California Senate Bill 100). After establishing a model, this paper analyzes options to achieve a fully renewable supply in the electricity sector alone. Sensitivities to operational constraints and possible alternatives are discussed, and a section investigates the hydrogen storage energy capacity issue. Moreover, an estimation of costs is provided. Subsequent papers will analyze the impact of sector integration, e.g., when a push for electrification occurs in the heating sector or when strong decarbonization is sought also in transportation.

Background

In recent years, the State of California has taken steps towards the decarbonization of its energy system by issuing multiple bills and passing many laws regarding renewable energy in the power sector, greenhouse gas (GHG) emissions control, and clean fuels for transportation. In September 2018, the Governor signed Senate Bill 100 (*100 Percent Clean Energy Act*) into law, thus officially establishing the objective of 100% clean and mostly renewable retail sales of electricity by 2045 [5]. Intermediate steps already codified into law are 33% renewable supply by 2020 and 50% by 2030. By 2020, California must reduce GHG emissions to 1990 levels and have 1 million zero-emission vehicles in service to comply with AB 32 [6] and SB 1275 [7], respectively. Renewable power generation and renewable fuels will aid compliance with these laws.

Decarbonizing the energy system is not just a California issue, but a global one. In the European Union, the clean energy directives impose 27% renewable supply on final energy consumption, which includes but is not limited to electricity, and a 40% cut in GHG emissions against 1990 levels by 2030 [8]. The long-term 2050 Roadmap states that an 80% GHG emissions reduction from 1990 levels is due by 2050, with power generation emissions expected to decrease as much as 99% to balance sectors like agriculture where reductions are necessarily smaller [2].

The combined issues of depleting fossil fuel reserves, air quality, geopolitical instabilities, and climate change are pushing both Western and Eastern countries to study the conversion of their power systems to high RES percentages. The recent drop in the cost of photovoltaic and wind power generation technologies [9,10] is also encouraging RES adoption. A roadmap integrating North Africa and Europe has developed a technologically feasible pathway to reach 100% RES electricity supply by 2050; but, it has identified how the realization depends upon government policy, market, investments, and new infrastructure challenges [11]. A theoretical study on Australia has applied an energy balance model that uses historical data for wind, sun, and electrical demand to determine hourly RES power generation, showing that transformation of the power sector to 100% RES is

possible [12]. To assess the possibility of satisfying the electrical demand with wind and solar sources in the United States, a long-term study has evaluated 36 years of global hourly data to determine mean annual values, which are then used to identify various combinations of wind and solar capacities capable of meeting 150% of the 2015 demand, where the additional 50% generation is taken to account for reliability of the grid [13]. Using an in-house developed energy system modeling tool, researchers at Lappeenranta University of Technology (LUT) have studied the integration of power, desalination, and non-energetic industrial gas sectors in various Eastern countries (India, Iran, Pakistan, and Saudi Arabia). The model optimizes the least-cost mix looking at annual costs of installed capacities of various RES, dependent upon the availability of wind speed, solar irradiation, and precipitation (from historical weather data). Results show that 100% RES coverage of demand in integrated sectors can be accomplished by predominately PV and wind resources by the year 2050 [14–17]. A study from Stanford University explored the potential for meeting not just electricity by economy-wide energy demands with hydro, solar, and wind resources in 139 countries around the world [18]. At an international agency level, the European Renewable Energy Council has analyzed the economic and technological challenges of renewables and has concluded that deploying RES technologies is a promising effort humans can make to reduce climate change's tremendous impact on their lives [19].

With the increase of RES capacity connected to the grid, the need for energy storage arises to avoid curtailment and manage supply to meet non-concurrent demand. Indeed, power generation from major RES such as wind and solar is unpredictable, hence difficulties with the instantaneous balance of electricity supply and demand occur already at present installation levels [20]. Energy storage options to assist in load balancing include pumped hydroelectric storage, battery energy storage systems (BESS), compressed air energy storage, and P2G. Among them, pumped hydro is a well-established technology, but has a strong dependence on geography and climate. BESS and P2G are the most studied alternatives in the energy industry for new applications. With recent battery cost reductions and technology maturity, BESS are the next most popular systems that are being installed around the world for balancing electricity supply and demand [21]. P2G consists of hydrogen generation via water electrolysis powered by excess electricity and offers the advantage of multiple possible pathways for hydrogen use, among others: direct use as fuel (allowing decarbonization of transportation), transformation into liquid or gaseous fuels/chemicals, and reconversion to electricity [22]. The latter can be more precisely referred to as Power-to-Power (P2P) or Power-to-Gas-to-Power (P2G2P) and it is the most relevant for electric grid support applications; it is typically obtained by coupling the electrolyzer with a fuel cell system through local or distributed hydrogen storage [23]. Importantly, BESS and P2G/P2P technologies powered by renewable electricity both offer zero GHG and zero criteria pollutant emissions features. They differ in the energy-to-power ratio (kWh/kW). Batteries have a constant and fixed energy-to-power ratio, so that large energy capacity inevitably leads to additional unnecessary power capacity that must be installed. P2G/P2P systems can accept and release any amount of energy while designing the electrolyzer power capacity to a desired level, since the power and energy quantities are independently determined (i.e., power scales with electrolyzer size and energy scales with hydrogen storage facility size). Although BESS have a high nominal efficiency, their operation has shown highly variable and low average round-trip efficiencies[1] around 50-55% in grid-support applications [24,25]. This relatively poor performance is due to cooling requirements (even during stand-by in the case of high-temperature batteries) and power conversion system parasitic loads that can perhaps be improved with modern BESS systems; but, it is also due to battery self-discharge, which is inevitable. Moreover, BESS used for large amounts of energy storage require a large land footprint and can become very costly [26], in addition to showing issues of reliability and lifetime [27]. P2G/P2P systems are interconnected with the electric grid through the same power conversion equipment (e.g., inverters) as BESS so that they can act just as rapidly to match supply and demand, while providing the same ancillary services. However, there are

[1] The round-trip efficiency of an energy storage system is defined as the ratio between the amount of energy withdrawn from and the amount of energy fed to the system, over a cycle that determines no variation of the stored energy. Reduction from input to output occurs due to losses during the charging and discharging processes, as well as consumption by auxiliaries to keep the balance-of-plant running and the self-discharge factor, where applicable.

issues about hydrogen storage, management, and distribution, and regulation uncertainty, in addition to relatively high costs due to the early market stage of P2G concepts.

Studies on the use of P2G have explored both small- and large-scale systems. A 1999 study evaluated a family home in Switzerland operating on a privately owned PV-hydrogen generation and storage system that had been run since 1991, thus verifying how P2G could be a technically viable solution for small scale energy storage applications [28]. Another residential-scale study of P2P for a California residence was completed in the early 2000s showing that grid-independent operation using a reversible fuel cell was possible [29,30]. Although small-scale systems are intriguing for residential energy management, large-scale P2G will be needed to attain the clean energy shift on a regional power grid or on a microgrid, as demonstrated also by recent EU project on grid-assisting proton exchange membrane (PEM) fuel cell power plants [31]. Recent work has looked at the possibility to integrate P2G with electrified heating (heat pumps) at urban scale, to reduce overall fossil fuel consumption [32]. Studies on whole countries (e.g., Spain [33] and Italy [34,35]) or regions (e.g., a Norwegian island [36] or an Alpine area [37]) have analyzed the integration of P2G at large scale. The Spanish study [33] used a numerical model to size the electrolyzers based upon the maximum power fed to them from wind and solar surplus energy, determined by historical load and wind and solar power profiles. The produced hydrogen is then used to reshape the power load curve by dynamic dispatch of a fuel cell. The Italian investigation [34] assessed the potential for P2G installation based upon a large increase in installed renewable power capacities, then comparing with Germany to show the differences in residual load profiles, and analyzing the recovered and curtailed energy related to high PV vs. high wind as main available resource. A second study on Italy [35] expanded the long-term analysis to sector integration and introduced a multi-node representation, assessing energy and environmental performance of different system evolution options based upon forecast scenarios with large RES installation and high shares of plug-in electric vehicles and fuel cell electric vehicles. In the study, hydrogen production recovers the excess electricity and provides a clean transportation fuel, seeking minimum curtailment rather than fully renewable supply, as the installed capacities are set from available forecasts and not solved by optimization.

Methods and models

This work proposes a model to simulate the power system behavior on large geographical scale, analyzing the effects of different installed RES capacities on the hourly system dynamics, looking at extended time frames (year-long behavior). Expected results include the estimation of power generation and energy storage capacities and dynamics needed to attain a very high share of renewable electricity supply. This study focuses on hydrogen as storage means, but no restriction to a specific storage technology is inherent in the model. Indeed, some simulations involve lithium-ion BESS, either as a complementary technology to deal with P2P capacity factor constraints or as the only option, for comparison.

Before discussing the methods and results, it is important to highlight that this kind of study involves a large set of assumptions, from plant efficiencies to simplification of grid topology. Due to that, the significance of investigating future system evolution does not lay in the exact values obtained as simulation results, but rather in general trends, orders of magnitude, and mutual comparison found for the investigated variables, with the final aim of assessing the potential role of hydrogen-based storage technologies. The main underlying assumption is the priority use of renewable generation plants and storage devices up to installed capacity and resource availability, besides market mechanisms where competition acts. Results give an overview on the installed capacity of generation and storage devices required to fulfil the very ambitious targets of the energy transition. Also, incentives and policies will play a crucial role and may influence or direct the technological development towards different solutions (for this purpose, the reader may refer to studies on the topic like [38]).

Modeling approach

The analyzed large-scale system includes electric loads, power plants, and storage devices as shown in Figure 1. The model uses a lumped approach that considers the structure as a single node, with all generation and consumption points interconnected with no transmission limitations (copper-plate power grid assumption). Power exchange with neighboring regions (e.g., a different Independent System Operator (ISO) area) is modeled, but it is assumed to contain zero renewable energy when entering into the system, so that it belongs to the 'non-RES power plants' generation. Power transmission to adjacent areas is not considered because the primary aim is to satisfy the internal demand with local renewable resources and adequate storage.

The model computes the balance of active power within the system at each time step, which is fixed to either 1 hour or 15 min, depending upon data availability (at least 1-hour resolution is available for all resources and demands considered).

Storage technologies considered are BESS and P2G/P2P. In its essential form, P2G is comprised of an electrolyzer for hydrogen production and a hydrogen storage tank; when coupled with a device that generates electric power from hydrogen (e.g., a fuel cell or a combustion-based engine like a gas turbine), the overall system is called Power-to-Power (P2P). While combustion turbines are currently less expensive [39], fuel cells exhibit higher efficiency (we are not referring in this comparison to the case of combined cycles, but rather to simple cycle gas turbines which are considered particularly suitable for very fast ramping grid support) and allow for generation of electricity at zero local and global emissions [40], so they are selected for this purpose in P2P designs.

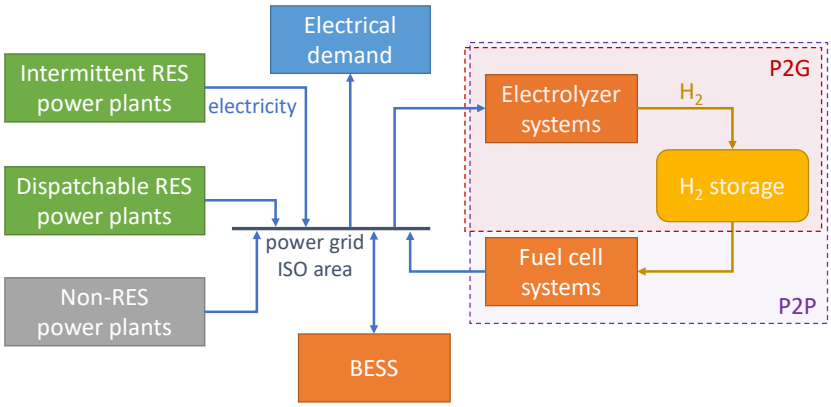

Figure 1 – Schematic of the power system structure that is simulated.

The simulation reproduces the supply-consumption electricity balance over each time interval, prioritizing the use of renewables up to the maximum output capability, for each generation type, based upon the installed capacity and the generation profile (e.g., temporal availability of wind and solar).

At each time step t, a balance equation is solved:

$$P_{RES,t} + \sum_s P^s_{out,t} + P_{other,t} = P_{load,t} + \sum_s P^s_{in,t} + P_{curt,t} \quad (1)$$

where $P_{load,t}$ is the electrical demand, and $P_{RES,t}$ is the generation from wind and solar power plants. For each storage technology s, $P^s_{out,t}$ and $P^s_{in,t}$ are the output and input power, respectively. The variable $P_{other,t}$ represents the additional generation that must be called in to satisfy the demand after direct use of renewables and extraction from storage. Although its value will be zero as a result of the simulations for 100% RES supply, it must be taken into account in the calculations. $P_{curt,t}$ is the overgeneration that cannot be accommodated by the storage.

The time evolution of the storage energy content, to be repeated for any storage technology s, is expressed by:

$$E^s_t = E^s_{t-1}(1 - \varepsilon^s_{sd}) + P^s_{in,t} \cdot \Delta t \cdot \eta^s_{in} - \frac{P^s_{out,t} \cdot \Delta t}{\eta^s_{out}} \quad (2)$$

where E_t^S is the energy content (kWh) at the end of time step t, Δt is the time step size, η_{in}^S and η_{out}^S are the charging and discharging efficiency, respectively, and ε_{sd}^S is the self-discharge coefficient applicable to the selected time step.

Model procedure

The computational procedure follows the schematic in Figure 2.

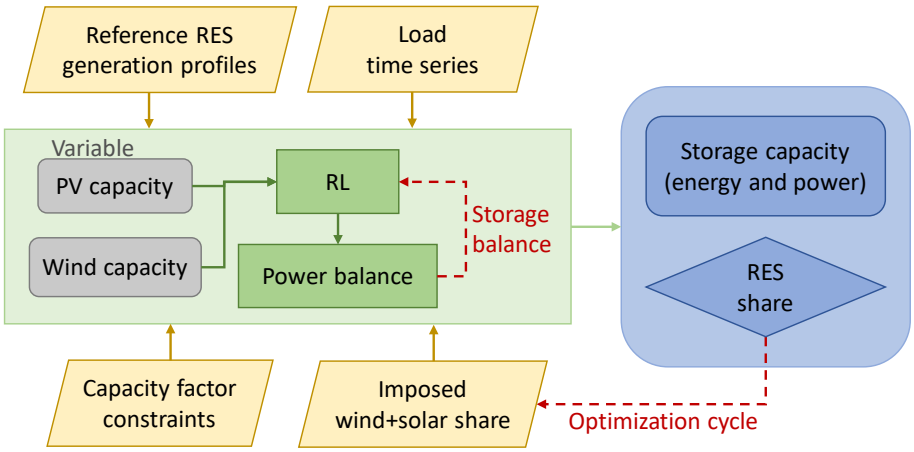

Figure 2 – Schematic of the model procedure.

First, the residual load RL is determined for each time step t as the difference between total load and RES generation:

$$RL_t = P_{load,t} - P_{RES,t} \tag{3}$$

The power generation profile of each renewable source i in the simulated case ('future') is obtained by linearly rescaling the corresponding historical one ('reference'):

$$P_{gen,i,t}^{future} = P_{gen,i,t}^{reference} \cdot \frac{P_{inst,i}^{future}}{P_{inst,i}^{reference}} \tag{4}$$

where $P_{gen,i,t}$ is the power generated at time t and $P_{inst,i}$ is the installed capacity. This approach maintains the value of the operating equivalent hours (EOH) of each technology, based on the consideration – not new in the literature [34,41] – that the capacity increment will enlarge installations at the currently exploited locations using improved technology, as the best areas have already been selected[2].

Second, the excess of generation (negative residual load) feeds the storage up to the installed capacity, and then is curtailed if the storage has reached maximum capacity. Any positive residual load is covered by extracting electricity from storage (considering appropriate conversion efficiency) or other dispatchable generation units. These are modeled to be any fast-ramping dispatchable plant that will be available as needed (e.g., natural gas- or biogas-fired combustion turbine), with no further technical detail, because the interest of the work is focused on analyzing 100% wind and solar renewable cases that avoid the contribution from these combustion-based technologies.

The system simulation occurs within an optimization cycle that seeks the minimum generation capacity needed to attain the desired RES share ($x_{RES,min}$), as described by Eq. 5. The RES share is defined as the ratio between RES electricity that meets demand (directly or through storage) and total electricity demand (line 4 in Eq. 5).

[2] This is particularly realistic for wind resources in California, which are concentrated in a few places, and which currently have older technology installed that cannot extract as much power from the same wind resource.

The optimization algorithm could solve wind and solar PV capacities together, setting the wind/PV capacity ratio in advance. To allow comparison of various combinations of technologies, simulations presented in this paper assume a given value of wind installed capacity, instead, and use the optimization routine to determine the solar PV capacity under the RES share requirement. The installed power capacities of the storage systems (line 7 in Eq. 5) are limited by the larger value of excess electricity occurring (from the RL time series) and by capacity factor (CF) constraints (see section *Energy storage system features*). A non-negative net balance of the storage content over the year is also imposed (hydrogen in P2P or electricity in BESS, line 8 in Eq. 5). Other input data are the electricity generation profiles to rescale (labeled 'reference' in Eq. 4) and the load profile.

$$min\left(P_{inst,RES}\right)\ s.t.\begin{cases} P_{inst,wind} \\ power\ balance\ (Eq.1)\ \ \forall t \\ storage\ balance\ (Eq.2)\ \ \forall t\ \forall s \\ \frac{\Sigma_t(P_{RES,t}-\Sigma_s P^s_{in,t}-P_{curt,t})\cdot\Delta t+\Sigma_t\Sigma_s P^s_{out,t}\cdot\Delta t}{\Sigma_t P_{load,t}\cdot\Delta t} \geq x_{RES,min} \\ P^s_{in,t}\ \leq P_{inst,s}\ \ \forall t\ \forall s \\ P^s_{out,t} \leq P_{inst,s}\ \ \forall t\ \forall s \\ P_{inst,s} = f(RL, min\ CF)\ \ \forall s \\ E^s_{t=end} \geq E^s_{t=start}\ \ \forall s \end{cases} \tag{5}$$

Energy storage system features

The profiles of generated and stored energy are used to calculate the storage size in terms of energy and power capacities: e.g., hydrogen, fuel cell, and electrolyzer capacities for P2P systems, or BESS energy and power capacities. For hydrogen storage, the minimum energy capacity is calculated as the maximum difference of stored hydrogen in the year-long profile. The storage power capacity depends upon the residual load profile resulting from the RES installed capacities and the imposed capacity factor constraints.

In absence of constraints, the P2G storage is capable of accepting all the excess power generation, avoiding any curtailment; hence, the power capacity of the electrolysis systems is equal to the largest peak of excess electricity generation from RES (absolute value of the negative residual load). The addition of constraints (e.g., required capacity factor) limits the installation to a total capacity that satisfies as much of the power requirement possible to achieve a set capacity factor. Analogously, fuel cell system nominal power is equal to either the maximum peak of positive residual load (unconstrained) or the power that guarantees the desired capacity factor (constrained). Note that inevitable curtailment results in the constrained cases, because increased installation of RES is required to meet the RES share when the storage systems are forced to have a minimum capacity factor.

The capacity factor (CF) is a parameter that summarizes the device utilization. It is defined as the ratio between the energy treated by the device and the maximum amount of energy that could possibly have been treated by that same device (i.e., operating at 100% rated power) in the time period considered, as follows:

$$CF = \frac{\sum_{t=0}^{end} P_t\cdot\Delta t}{P_{inst}\cdot T} \tag{6}$$

where, considering an electrolyzer as example, P_t is the power sent to the device at time t, Δt is the size of a time step, P_{inst} is the electrolyzer installed capacity, and T is the total time period simulated.

An alternative quantity that conveys the same type of information is the equivalent operating hours (EOH), which expresses the time (number of hours) that the equipment should have run at nominal power to treat the same total amount of energy that they actually treated over the total time period. It is also referred to as equivalent full-load hours (EFLH). It is equal to the ratio between the total energy treated and the installed capacity, as follows:

$$EOH\ \left[\frac{h}{y}\right] = \frac{\sum_{t=0}^{end} P_t\cdot\Delta t}{P_{inst}} \tag{7}$$

An additional parameter that helps to define the feasibility of installing a device is the actual full-load hours (AFLH), which correspond to the time (number of hours per year) during which the devices operate at nominal power. A high AFLH characterizes installations whose nominal capacity is frequently exploited, thus helping achieve a high CF. To have an equivalent parameter that is expressed in relative terms, we also introduce the minimum capacity factor (min CF), which is defined as the smallest hourly capacity factor that may occur in any time step. As example, a 10% min CF corresponds to 876 AFLH. If we consider the excess electricity duration curves before setting the electrolyzers nominal power, imposing a minimum capacity factor leads to an installed electrolysis capacity equal to the negative residual load (in absolute value) whose occurrence (in percentage of total time) is numerically equal to the minimum capacity factor itself. Based on this definition, the P2G capacity can be identified by means of percentiles over the statistical distribution of values in the residual load profile, whose calculation is aided by the constant duration of the time steps.

The CF and the min CF are related but distinct parameters. In particular, the obtained average CF over a year is expected to be larger than the set min CF. This is coherent with the lumped approach used, especially for modular systems that are characteristic of batteries, fuel cells, and electrolyzers: that is, the GW-scale total installed capacity (equal to the maximum power treated, even if only for one time step) is the sum of multiple kW- or MW-scale devices, where guaranteeing a min CF means that no device is present that runs for an extremely short period of time. In real applications, actual frequency of full- and part-load operation varies, hence each unit will have a different CF and dispatching methods control the overall system.

A similar approach can be adopted for BESS, although only one value of power capacity is defined for both input and output. Moreover, the existence of a fixed ratio between energy and power capacities might require oversizing one of the two values to satisfy the storage demand.

Note that, for any technology, applying a constraint on the storage-to-grid power capacity may lead to conditions in which it is impossible to satisfy the demand, as some rare load peaks could be greater than the allowed installed capacity.

Data and assumptions

Currently, the California electricity grid features about 6 GW of wind plants and 9 GW of utility-scale solar PV systems; behind-the-meter rooftop PV systems account for an additional 7 GW, hence a total solar PV capacity of 16 GW (end of 2017) [42,43]. Evolution of the installed capacities from 2010 is presented in Table 1, together with the estimated technical potential. The wind capacity value is evaluated combining available land area that guarantees a gross capacity factor above 35% (at 140 m hub height) [44] with 5-MW on-shore turbines and average capacity density of 4 MW/km^2. Based on available land and solar irradiation, the potential for utility-scale solar PV has been estimated at over 4 TW, considering an average capacity density of 48 MW/km^2 [45]. Both evaluations exclude built environment and natural protected areas. The potential for rooftop PV amounts to 76 GW on small buildings, or 129 GW when considering all building types [45,46]. Existing concentrated solar power (CSP) plants in California have a total nominal power of 1.3 GW, mostly made of solar tower systems. Noticeably, no new capacity has been added since 2014 [43].

Table 1 – Recent evolution of installed capacity and estimated potential of RES power plants in California [43–45,47].

	2010	2015	2016	2017	Technical potential
Wind	3.18 GW	5.73 GW	5.73 GW	5.85 GW	231 GW
Solar PV (utility scale)	0.12 GW	6.08 GW	8.62 GW	9.39 GW	> 4 TW
Solar PV (rooftop)	n/a	3.90 GW	5.26 GW	6.60 GW	129 GW
CSP	0.41 GW	1.29 GW	1.25 GW	1.25 GW	undefined

The historical profiles used as reference by the model are taken from the California Independent System Operator (CAISO) [4] for the year 2016, and rescaled as described in section *Model procedure*.

This work focuses on wind and solar as power generation. Existing behind-the-meter PV rooftop systems are accounted for as changes in the load (the available data from the transmission system operator is the net load). Nonetheless, the scaled solar profiles deployed could well simulate either transmission integrated systems or a combination of these with behind-the-meter PV. The calculations do not aim at determining the detailed dispatch of the future grid, but rather at offering an estimate of the magnitudes of the generation and storage capacities required for the transition to a clean power grid. The actual evolution will surely be more complex, and other renewable resources like hydro, biomass, and geothermal will play a role; but, they are not discussed here either because a small increment is foreseen (e.g., hydro and geothermal) or because their dispatchability makes them relevant for peak and reserve demand that are not investigated (e.g., biomass and biofuels).

Storage involves P2G and BESS, either exclusively or in combination, looking at best available technologies and future predictions for performance parameters. The assumed efficiency of hydrogen generation from electricity is 65%, based on lower heating value (LHV) [48]. The main available technologies for electricity generation from hydrogen are fuel cells, gas turbines (as simple or combined cycles), or internal combustion engines. The first option has been in the spotlight lately and is undergoing intense research and development, at the moment featuring higher efficiency at higher cost [39]; the second and third choices are well-established devices that could be repurposed to hydrogen fuel. This work selects PEM fuel cell systems for electrical generation from the stored hydrogen, due to high efficiency and good fast-ramping capability. All losses involved with hydrogen storage (e.g., compression and cooling) are included in the electrolyzer and fuel cell efficiency values used. Possible self-discharge losses correspond to hydrogen leakage from tanks, pipes, or reservoirs. These leakage losses are neglected here, as both the studies on Lined Rock Caverns (LRC) [49] and the available measures from existing underground facilities have shown very low leakage rates (further investigation is expected with operation of the first installations, e.g., in the Houston, Texas area) [50]. Although nominal efficiency for batteries is usually given as high as 95% in charging and discharging, data from grid-connected BESS that include parasitic losses of transformation and cooling have shown smaller values (e.g., average round-trip efficiency between 44% and 74% [24,25]). To account for this while considering future expected improvements, BESS are modeled with a 75% round-trip efficiency. Furthermore, a self-discharge factor of 5% per month is taken into account to better represent the physical and electrochemical processes occurring within BESS. Relevant parameters of the considered storage technologies are listed in Table 2.

Table 2 – Efficiency values for the various storage systems.

Parameter	*Value*	*Ref.*
Electrolyzer efficiency (LHV)	65 %	[48]
Fuel cell efficiency (LHV)	64 %	[51]
BESS round-trip efficiency	75 %	Own assumption, based on [24,25]
BESS efficiency in	87 %	Own assumption, based on [24,25]
BESS efficiency out	87 %	Own assumption, based on [24,25]
BESS self-discharge	5 %/month	[52]

A fully renewable power system

The developed model is applied to the California power system, based on data and assumptions defined in section *Data and assumptions*. The optimization routine first identifies different combinations of wind and solar

installed capacities that are able to meet 100% renewable coverage of the annual electricity demand, using P2P as energy storage technology. Then, varied capacity needs are compared after the model constrains the use of electrolyzer and fuel cell systems to guarantee reasonable capacity factors. As comparison, storage capacity requirements in the alternative case of lithium-ion BESS are estimated for meeting the same electrical system demand over the year.

All cases involve the use of solar and wind as power generation sources, and deploy hydrogen storage (using electrolyzers and fuel cells) or battery storage systems. CSP plants are taken into account with an installed capacity equal to present value (1.25 GW). All solar capacity additions are considered to be PV panels (the least expensive option available today). Load values and the dynamics of electricity demand are assumed unchanged with respect to 2016 data. This is reasonable since electricity demand has been relatively flat in California for the last 20 years due to a combination of energy efficiency measures and less electricity-intensive industry that counterbalances increased population and economy. Hence, the results give the values of the required increase in RES capacity that would be required to switch to a fully renewable system in the short term, or, if current trends of relatively constant demand persist. In the long term, electric mobility, electrification of loads, or other major technology shifts may change both total consumption and hourly load profiles – these aspects will be the bases for future study.

Unconstrained energy storage systems installation

The first set of simulations looks for combinations of wind and solar PV installed capacities that allow a fully renewable supply of electricity in the state when no constraints are imposed on electrolyzer systems. The sizing of the hydrogen-generating devices assumes that their total installed capacity equals the greatest absolute value of the negative residual load that occurs during any one hour along the year, thus recovering all excess electricity and excluding curtailment. Analogously, the use of fuel cell systems is not constrained and their sizing results from the need to satisfy the demand at any rate, hence their power capacity corresponds to the highest value of positive residual load.

Figure 3 depicts a set of 12 possible combinations, for wind capacity up to 120 GW (around half of the estimated potential in California). As expected, the more wind that is included in the electricity production mix, the less solar PV is needed. However, intermediate cases present a lower total installed power of RES plants and also smaller electrolysis system capacity, thus showing that a combined use of solar and wind power would be most effective for meeting annual demand. Indeed, P2G electrolyzer power capacity has a minimum, equal to 55 GW, in Case 8, which also features the lowest total installed RES capacity (80 GW wind and 37 GW PV). Very similar values of electrolysis and total RES capacities are found in Case 9 (90 GW wind and 27 GW), with differences below 0.2%. Fuel cell system power capacity is mainly determined by the positive residual load (i.e., power demand unsatisfied by direct use of RES generation) rather than by the energy consumption to be supplied by the storage, and the required value does not vary significantly (30 to 37 GW). Power generation sizing does not change much because the likelihood that one night-time hour of the year possesses nearly zero wind power is high, leading to minimum power capacity that is close to the average night-time load.

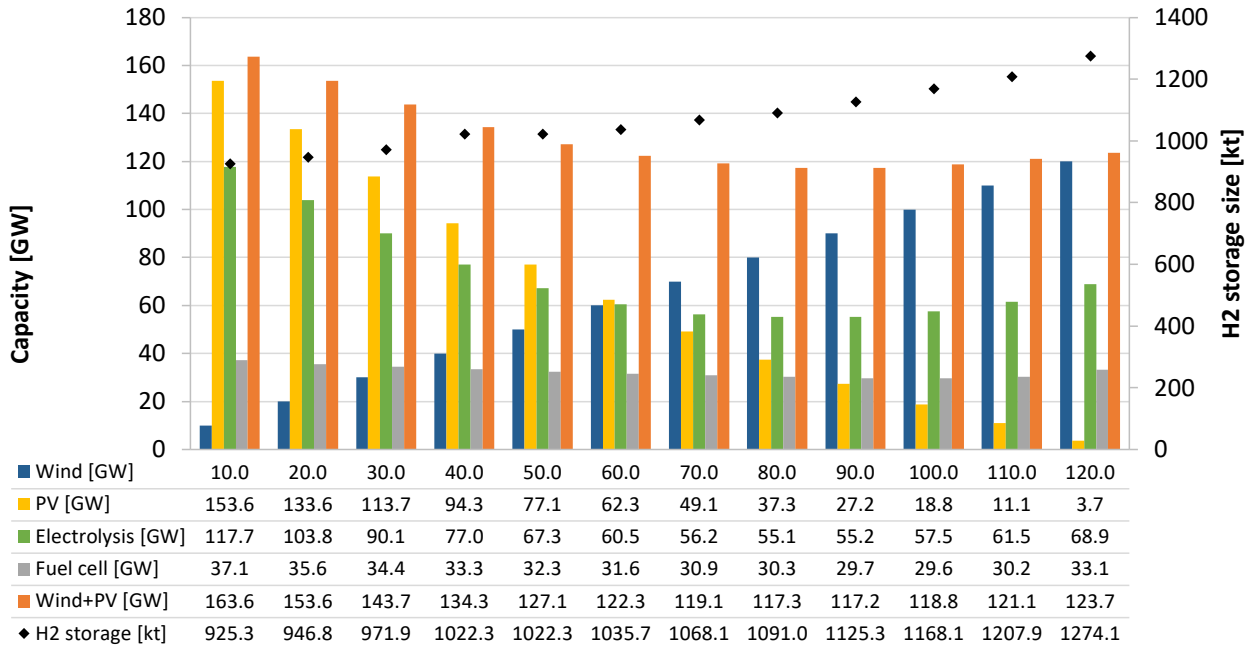

Wind [GW]	10.0	20.0	30.0	40.0	50.0	60.0	70.0	80.0	90.0	100.0	110.0	120.0
PV [GW]	153.6	133.6	113.7	94.3	77.1	62.3	49.1	37.3	27.2	18.8	11.1	3.7
Electrolysis [GW]	117.7	103.8	90.1	77.0	67.3	60.5	56.2	55.1	55.2	57.5	61.5	68.9
Fuel cell [GW]	37.1	35.6	34.4	33.3	32.3	31.6	30.9	30.3	29.7	29.6	30.2	33.1
Wind+PV [GW]	163.6	153.6	143.7	134.3	127.1	122.3	119.1	117.3	117.2	118.8	121.1	123.7
H2 storage [kt]	925.3	946.8	971.9	1022.3	1022.3	1035.7	1068.1	1091.0	1125.3	1168.1	1207.9	1274.1

Figure 3 – Set of combinations of capacities (generation and storage) that are each able to achieve 100% RES electricity supply with P2P as storage technology.

The constraint of non-negative net hydrogen generation over the year guarantees that hydrogen is available at the end of the simulated period to repeat the system behavior in the subsequent year. In case of positive net production, part of the stored fuel is in excess of the operational needs, so it is available for different uses (e.g., fuel for hydrogen transportation, feedstock for industrial processes). The excess hydrogen is a result of the numerical convergence of the optimization procedure and is nearly zero in all cases of this set of simulations (thus allowing a fair comparison), meaning that the installed capacities are just right to guarantee the overall balance. The black diamond markers in Figure 3 represent the minimum hydrogen storage size required to guarantee the yearly functioning of the system, referred to the right axis. Storage needs increase when the combination of wind and PV capacity is shifted towards the first, up to about a 30% higher capacity needed. Section *Hydrogen storage capacity* further discusses energy capacity needs.

Constrained electrolyzer installation and capacity factor

The calculations performed in the previous section assume unconstrained use of electrolyzers for P2G, meaning that no minimum load is assigned nor minimum capacity factor is imposed. While the former deals with a single-device analysis which is out of the scope of this large-scale analysis, the latter is relevant as no facility is reasonably expected to be installed if it is to operate only for a very short amount of time. Indeed, recovering all the excess electricity generated by wind and solar plants leads to very steep load duration curves for the electrolyzers, as shown in Figure 4 for four selected cases. To accommodate such amounts of power, the devices would have to be sized with large power capacity, part of which will be used only for a very limited amount of time (e.g., a capacity of more than 20 GW operates in less than 10% of the total time in the case '10 GW wind - 154 GW PV'). On the opposite end of the x-axis in Figure 4, the fraction of time above which the duration curve flattens to zero depends upon the solar/wind ratio, as it represents the absence of excess electricity. The cases featuring low wind capacity and large PV installation have a natural limitation for 50% of the total time, as solar generation is only present for one-half day at most, while high-wind cases produce longer operating times for the electrolyzers. The lowest overall curve is obtained at 80 GW wind and 37 GW, which also has one of the lowest total RES installed capacity.

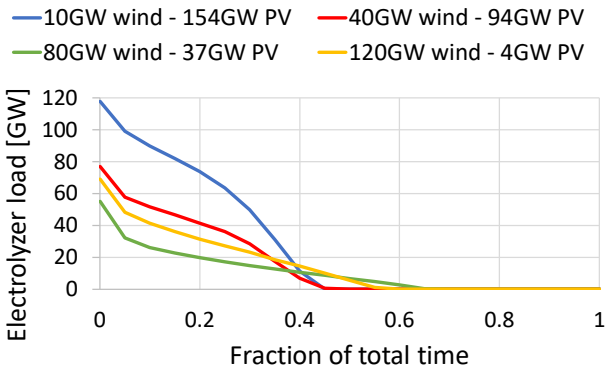

Figure 4 – Electrolyzer system load duration curve when they treat all excess electricity from wind and solar, in four selected cases.

This section investigates how constraints on electrolyzer system operation affect the system ability to reach a fully-RES-based power sector, by performing a sensitivity analysis on the electrolysis system capacity factor.

Figure 5 shows the electrolyzer system load duration curve at various minimum CF in two example cases of very low and very high wind capacity (10 GW and 120 GW, respectively). Cases with intermediate values of assigned wind capacity have analogous behavior when varying the constraint (appearing of a cap on capacity that increases at greater minimum CF), with differences in the absolute values and in the curve shape as outlined in Figure 4 for the unconstrained simulations. The effect of imposing a minimum capacity factor is straightforward: the power fed to the electrolyzers plateaus at a certain value that corresponds to the installed capacity, which numerically equals the load curve value of the assigned min CF. The overall shape of the curve does not vary significantly when increasing the min CF, but some differences exist as the reduction of electrolysis capacity impacts the hourly balances, by decreasing the availability of stored fuel and therefore increasing the need for RES installation. The right shift of the curves represents the increase in excess electricity recovery due to larger PV capacity (and then excess generation) at given installed wind power capacity.

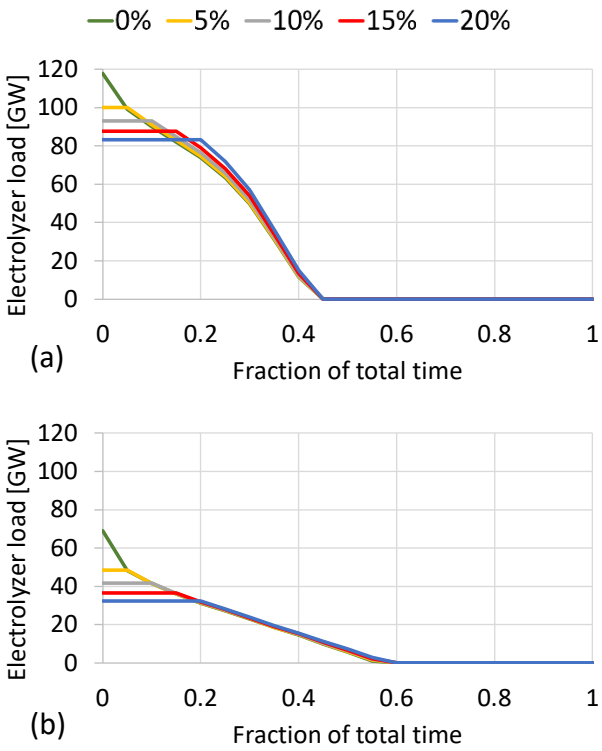

Figure 5 - Electrolyzer system load duration curve, at different imposed min CF for electrolyzers sizing, in the two cases of wind capacity at: (a) 10 GW and (b) 120 GW.

For the overall system, the presence of a constraint on P2G installation determines greater RES capacities to guarantee 100% clean electricity supply. Figure 6 depicts the values of generation and storage installed capacities at different imposed min CF on the electrolyzers, in four selected cases that feature small, moderate, large, or very large increases in wind capacity (10, 40, 80, or 120 GW, respectively). In these simulations, the fuel cell system nominal power is not restricted, so it is equal to the peak positive residual load. The variation of installed electrolysis capacity features a big step when first introducing a limitation (from 0% to 5% min CF) and is smaller thereafter. From a no-limitation case to a 20% min CF case, the electrolyzer system installed capacity decreases by 29-38% in the low-wind cases, while PV installed capacity increases only by about 9%. In the 80 GW case, a 60% electrolysis power capacity reduction is obtained with a 17% increment of PV nominal power. With 120 GW wind, the P2G system size could be halved if 5 GW of PV are added to the system – this corresponds to more than doubling the PV installation, but the total value is rather small compared with the quantities under consideration. Fuel cell system capacity does not vary with the assigned minimum electrolyzer CF due to the direct correlation to the positive residual load, which is only slightly affected by the small variations seen in the installed RES capacity. The 120 GW wind case is an exception to this. It can be explained by the high relative variation of PV capacity, which makes a significant profile change. Note that this analysis suggests that some amount of renewable energy installation that is greater than that required to meet RES goals – which leads to some curtailment of RES power, but much smaller energy storage systems – is likely the lowest cost option.

The black diamonds in Figure 6 represent the electrolyzer average capacity factor, referred to the right axis. As expected, this quantity is always higher than the imposed minimum CF, and it increases when the latter increases. In absence of constraints, the average CF stabilizes around 20% (corresponding to 1800 EOH). When imposing a 10% minimum capacity factor, the average CF ranges from 30 to 36% (2600-3200 EOH). With an assigned 20% min CF, the average CF is always over 33% and peaks at 45% (almost 4000 EOH) in the case featuring 80 GW wind capacity. In general, smaller P2G capacity values come from the 80 GW wind capacity cases, which also feature higher average CF; this is due to a high wind/PV ratio that determines lower excess

electricity peaks due to the semi-complementary solar and wind dynamics, as observed also with unconstrained electrolyzers.

Figure 6 also presents the RES electricity curtailment, i.e., the excess RES electricity that is not recovered by P2G and therefore lost. RES electricity curtailment is presented as absolute values (in the tables) and as a fraction of the total excess electricity (both in tables and as red dots in the graphs, referred to the right axis). Inevitably, the values increase when the minimum CF increases. The highest amounts of lost electricity occur in the low-wind case, while the greatest relative losses are in the 80 GW wind case, which also corresponds to the smallest installed capacities (both RES plants and P2G electrolyzers) and the lowest amounts of excess electricity.

(a)

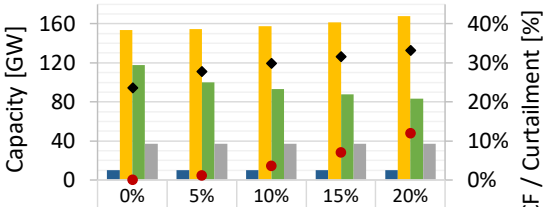

	0%	5%	10%	15%	20%
Wind [GW]	10.0	10.0	10.0	10.0	10.0
PV [GW]	153.6	154.8	157.4	161.4	167.8
P2G [GW]	117.7	100.0	93.0	87.7	83.2
FC [GW]	37.1	37.1	37.1	37.1	37.1
Avg CF [%]	23.6%	27.7%	29.8%	31.6%	33.2%
Curtail [%]	0.0%	1.1%	3.5%	7.0%	11.9%
Curtail [TWh]	0.0	2.8	8.9	18.2	32.9

(b)

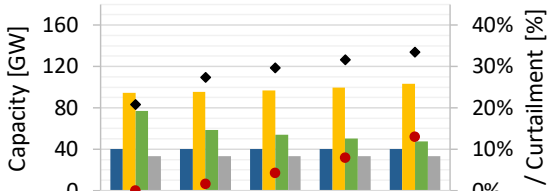

	0%	5%	10%	15%	20%
Wind [GW]	40.0	40.0	40.0	40.0	40.0
PV [GW]	94.3	95.3	96.9	99.5	103.2
P2G [GW]	77.0	58.4	53.8	50.4	47.5
FC [GW]	33.3	33.3	33.3	33.3	33.3
Avg CF [%]	20.8%	27.4%	29.7%	31.6%	33.4%
Curtail [TWh]	0.0	2.2	6.1	12.1	20.8
Curtail [%]	0.0%	1.6%	4.2%	7.9%	13.0%

(c)

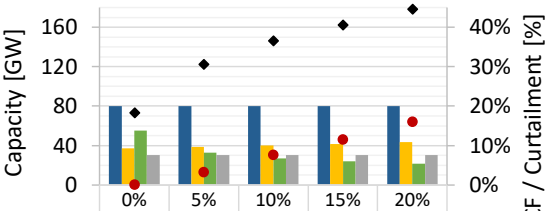

	0%	5%	10%	15%	20%
Wind [GW]	80.0	80.0	80.0	80.0	80.0
PV [GW]	37.3	38.4	40.0	41.6	43.6
P2G [GW]	55.1	32.6	27.0	24.1	21.7
FC [GW]	30.3	30.3	30.3	30.3	30.3
Avg CF [%]	18.2%	30.5%	36.5%	40.6%	44.5%
Curtail [TWh]	0.0	2.8	7.0	11.1	16.1
Curtail [%]	0.0%	3.1%	7.5%	11.4%	15.9%

(d)

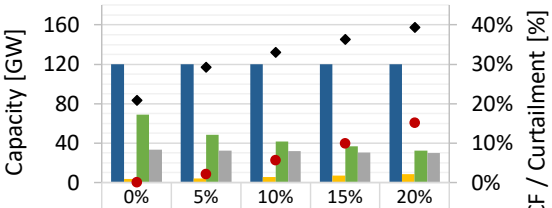

	0%	5%	10%	15%	20%
Wind [GW]	120.0	120.0	120.0	120.0	120.0
PV [GW]	3.7	4.4	5.5	6.9	8.8
P2G [GW]	68.9	48.4	41.6	36.7	32.2
FC [GW]	33.1	32.6	31.7	30.6	30.0
Avg CF [%]	20.8%	29.2%	33.0%	36.2%	39.4%
Curtail [TWh]	0.0	2.7	7.1	12.7	19.9
Curtail [%]	0.0%	2.1%	5.6%	9.8%	15.2%

Figure 6 – Power system characteristics at different imposed min CF for electrolyzer system sizing, in the four cases of wind capacity at: (a) 10 GW, (b) 40 GW, (c) 80 GW, and (d) 120 GW. Left axis: installed capacity of generation and storage; right axis: average electrolyzer capacity factor and curtailed electricity (as fraction of the excess generation after direct use of RES).

Constrained fuel cell installation and capacity factor

As was the case for the electrolyzer systems, fuel cell system installation may become uneconomical in case of underutilized capacity, i.e., low capacity factor. As an example, the green lines in the graphs of Figure 7 represent the load duration curve of fuel cell systems in absence of capacity factor constraints. The curve shape varies with the wind/PV ratio, but a steep drop can be noticed between 0 and 5% of the total time in all cases, corresponding to about 10 GW of installed capacity used for less than 400 hours per year.

This section analyzes the effects of constraining the installation of fuel cells with a minimum capacity factor. All the definitions introduced in section *Energy storage system features* and the remarks noted for constrained

electrolysis systems apply, with the difference that here the energy flows are the fuel cell system output and not the electrolyzer system input.

Imposing a min CF on the fuel cell systems limits their installed capacity to a nominal power smaller than the highest peaks of positive residual load seen on the grid; therefore, it is impossible to satisfy 100% of the state electrical demand with any combination of wind, solar, and P2P. This leads to the need for either a complementary dispatchable generation device or an additional storage technology. The first could be a conventional combustion-based power plant (e.g., internal combustion engine, gas turbine, or combined cycle, depending on the EOH) fed with either fossil or renewable fuels (e.g., natural gas, the P2G-produced hydrogen, biomass, or biogas). The second option involves mainly BESS, which is the option considered here. This set of devices will have a low CF, as they are only required to cover the small fraction of demand that is unmet by the fuel cell systems. The drivers for the choice of storage or generation technology will most probably include the investment cost and the technical features, as well as the capability to dispatch other grid services that are not investigated here.

We assume to feed BESS with excess renewable electricity not absorbed by electrolyzers. Total BESS power capacity depends upon the most limiting value between energy storage capacity needs and maximum power output required. The model implicitly assumes that P2G systems are sized independently of BESS and that P2P is always fed first by excess electricity, up to the electrolysis capacity. The simulation results presented in this section assume a 20% min CF (over 1750 AFLH) for the electrolyzer systems, which is well above the reference breakeven point (1000 AFLH) considered in literature when assuming mid-term prospective investment cost of electrolyzers [53].

Figure 7 shows the load duration curves resulting from the simulations under the assigned min CF for fuel cell system installation. The main effect is analogous to that seen for electrolysis devices in Figure 5. That is, for a fraction of time equal in value to the assigned minimum capacity factor, the fuel cells operates at constant load. Qualitatively, the reduction of the underlying area with respect to the green line (unconstrained case) represents BESS intervention to close the energy balance.

Figure 8 depicts the variation in installed capacity of PV plants, electrolysis systems, fuel cell systems, and BESS as a function of the min CF assigned. As expected, the fuel cell system power capacity decreases when installation is constrained, while BESS come into the picture. Opposite to what happens for the electrolyzers, stricter constraints on fuel cell CF reduce the required RES power generation capacity. This is due to the presence of constrained electrolyzer system installation, so that the introduction of BESS helps recover part of the curtailed excess electricity. However, the BESS energy capacity rises quickly as the fuel cell system constraint increases. The reduction of P2P capacity is small with respect to electrolyzer system capacity (-3% to -13%), because they are already limited by the 20% min CF, whereas the fuel cell system installed capacity decreases more than 50%. At the same time, PV capacity varies within 4-9% in low-wind cases, while it halves in the very high wind case. The need for BESS energy capacity reaches up to 7 TWh when the fuel cell systems are constrained to guarantee 1750 AFLH (20% min CF). Halving the requirement (10% min CF, 900 AFLH) reduces BESS energy capacity by about 70%. The BESS power capacity depends upon the energy-to-power ratio of the specific technology (e.g., in range 2-10 for lithium-ion batteries); however, it is never a limiting factor as it only has to match the residual load after P2P, which is below 20 GW even at 20% imposed min CF on fuel cell system sizing.

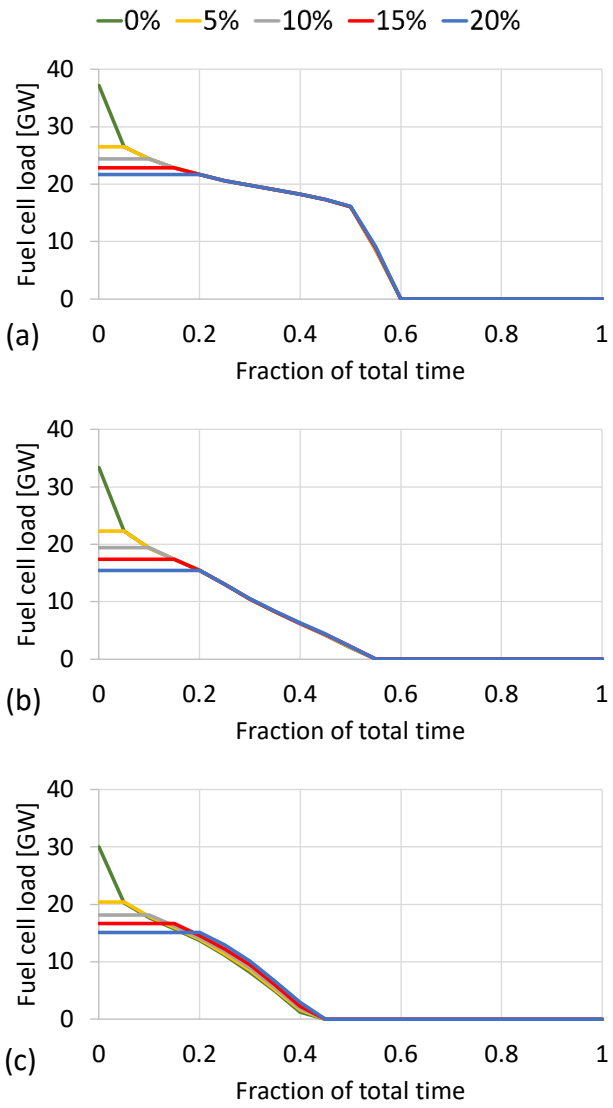

Figure 7 - Fuel cell load duration curve, at different imposed min CF for fuel cells sizing, in the three cases of wind capacity of: (a) 10 GW, (b) 40 GW, and (c) 120 GW.

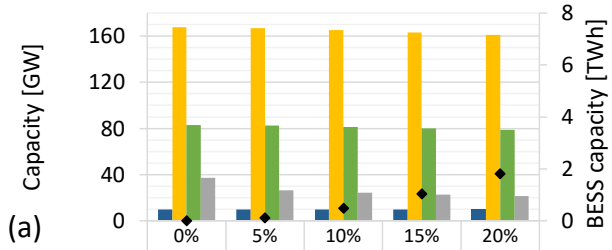

(a)

	0%	5%	10%	15%	20%
Wind [GW]	10.0	10.0	10.0	10.0	10.0
PV [GW]	167.8	166.7	165.1	163.2	161.1
P2G [GW]	83.2	82.5	81.5	80.2	78.9
FC [GW]	37.1	26.5	24.4	22.9	21.7
◆ BESS [TWh]	0.00	0.11	0.48	1.04	1.81
Avg CF FC	30.9%	43.0%	46.0%	48.3%	50.1%

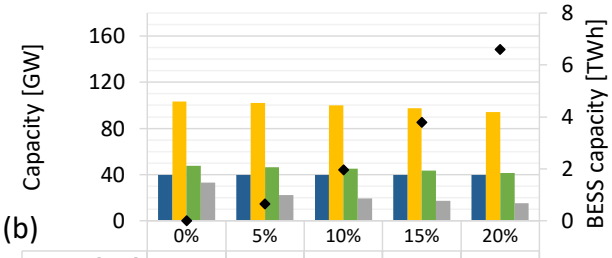

(b)

	0%	5%	10%	15%	20%
Wind [GW]	40.0	40.0	40	40.0	40.0
PV [GW]	103.2	101.9	99.8	97.4	94.2
P2G [GW]	47.5	46.6	45.2	43.6	41.4
FC [GW]	33.3	22.3	19.4	17.4	15.5
◆ BESS [TWh]	0.00	0.66	1.96	3.78	6.59
Avg CF FC	19.8%	29.0%	32.4%	34.7%	37.0%

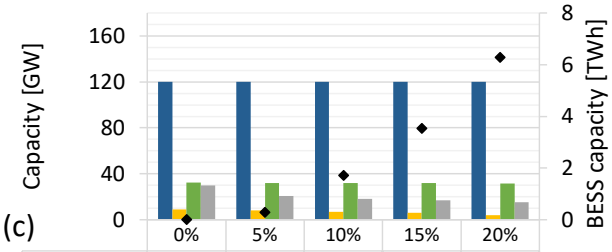

(c)

	0%	5%	10%	15%	20%
Wind [GW]	120.0	120.0	120.0	120.0	120.0
PV [GW]	8.8	7.9	7.0	5.8	3.9
P2G [GW]	32.2	32.1	31.9	31.7	31.3
FC [GW]	30.0	20.4	18.2	16.6	15.1
◆ BESS [TWh]	0.00	0.27	1.70	3.53	6.27
Avg CF FC	17.6%	25.7%	28.5%	30.8%	33.2%

Figure 8 - Power system characteristics at different imposed min CF for fuel cell system sizing, in the three cases of wind capacity at: (a) 10 GW, (b) 40 GW, and (c) 120 GW. Left axis: installed capacity of generation and storage; right axis: BESS energy capacity.

Comparison to BESS

As a comparison exercise, the option of entirely substituting the proposed P2P systems with BESS is investigated. The same optimization routine is used, imposing zero installed capacity of electrolyzer and fuel cell systems. The same assumptions on performance parameters and system dynamics apply. No additional constraints are imposed upon BESS operation, as the system relies solely on them to guarantee the hourly electricity balance. The simulations identify combinations of wind, solar, and BESS capacities that guarantee 100% renewable supply of electrical demand, minimizing the generation capacity and determining the needed storage capacity. In addition, sensitivity of the required BESS energy capacity to variations in the installed power generation capacity is analyzed: a second set of simulations is run that set wind and PV installed capacities

above the minimum values previously identified, replacing the objective function of the optimization with the minimization of BESS capacity. As expected, results depict a reduction of BESS energy capacity when greater power generation is present and curtailment is allowed.

Figure 9 displays the results, with the BESS energy capacity identified by the color scale. Points on the black line represents the case of minimum PV installation for a given wind capacity. As was the case for hydrogen-based storage, a high wind/PV ratio among these solutions increases the storage energy capacity needed due to the less regular profile of wind compared to solar. The white area contains combinations of RES capacities that are not able to satisfy the RES share requirement, independently of how large BESS capacity is introduced. Points in the colored area in Figure 9 represent combinations of capacities that meet the RES share requirement with smaller BESS, while enlarging the need for wind and solar installation. Here, curtailment is present, or excess storage filling occurs (i.e., net variation of energy content is positive over the year). Contrary to P2G options, where excess hydrogen production could be exploited for other uses (e.g., as fuel or feedstock), this electricity cannot be easily redirected to other purposes, since the electrical demand is already fully satisfied.

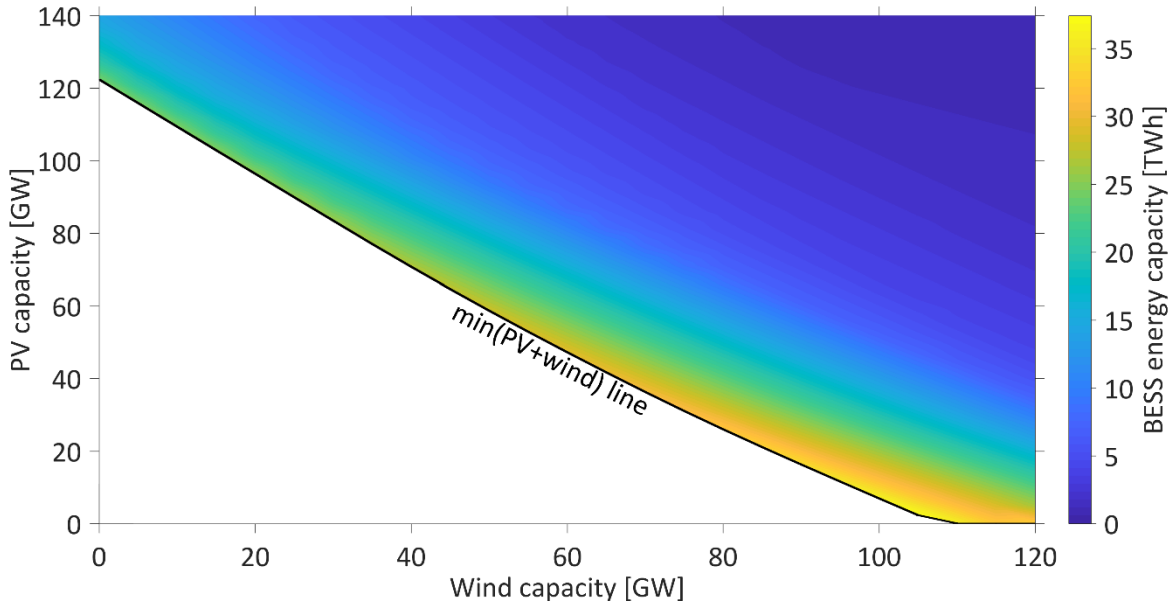

Figure 9 – Set of combinations of capacities (generation and storage devices) that are each able to guarantee 100% RES electricity supply with BESS as storage technology.

The exclusive use of BESS allows reducing the RES installed capacity compared to the P2P cases. However, the size of the required battery installation is very large. In the simulations at minimum RES capacity (black line in Figure 9), the PV capacity with BESS is 24-40% smaller than with P2P (excluding the very high wind cases where it falls to zero). At the same time, the required BESS capacity ranges from 24 TWh in high-solar cases to 37 TWh in wind-dominated cases. Table 3 compares the generation and storage capacities needed for 100% renewable electricity when alternatively using BESS or P2P. In general, the BESS size increases when the total RES installed capacity decreases, while electrolyzer systems do the opposite. This is due to the different sizing method: BESS installation is mainly driven by the energy capacity requirements, whereas the relevant parameter to size the electrolyzer systems is the excess power generation. Interestingly, the amount of BESS obtained here is fully comparable with the values reported by [27] through a different approach.

The resulting utilization factor of BESS (measured as equivalent operating cycles per year, EOC[3]) is really low: no case along the black line in Figure 9 features more than 7 EOC and the highest value in the whole plot is around 40 EOC, found in correspondence of 85 GW wind, 140 GW PV, and 1.1 TWh BESS capacities.

[3] The EOC is equal to the ratio between the total energy input and the energy capacity.

Table 3 – Comparison of installed capacities of PV and storage in the two alternatives of P2P or BESS as exclusive technology for storage, in five cases of assigned wind capacity.

Wind capacity	***P2P storage***		***BESS storage***	
	PV capacity	***Electrolysis capacity***	***PV capacity***	***BESS capacity***
10 GW	153.6 GW	117.7 GW	109.3 GW	24.8 TWh
40 GW	94.3 GW	77.0 GW	70.7 GW	27.0 TWh
80 GW	37.3 GW	55.1 GW	26.0 GW	32.4 TWh
100 GW	18.8 GW	57.5 GW	6.9 GW	36.4 TWh
120 GW	3.7 GW	68.9 GW	0.0 GW	32.8 TWh

Varying the RES share requirement

Although decarbonization of the power sector is a key step for GHG emissions reduction and large use of RES is an effective way to approach it, the proposal of '100% supply by wind and solar' might look like a very ambitious goal, which could be lowered when taking into account other options (e.g., bioenergy, waste-to-energy, carbon capture). Furthermore, even if the PEM electrolysis itself has demonstrated the ability to offer a wide range of grid services [54], flexibility and reserve requirements may require longer to switch away from conventional dispatchable plants, like gas turbines and combined cycles.

A sensitivity analysis evaluates the variation in the required installation of wind, solar, and P2P storage when setting the RES share to values below 100% (e.g., 80% or 90% of total demand). For this analysis, no capacity factor constraint is applied to the electrolyzer systems. As the constraint of full demand coverage by wind and solar is removed, the installed capacity and the operation of fuel cell systems are no longer a direct consequence of residual load profile and hydrogen availability, but they rather depend upon the dispatch, which is also related to the operation of the other dispatchable power plants ('dispatchable RES' and 'non-RES' in Figure 1). The model focuses then on cumulative quantities. The optimization routine constrains the fraction of total RES electricity delivered (sum of direct use and P2P reconversion) over the total demand to be greater than or equal to the required share. The generation and load hourly profiles determine the direct use of electricity or its redirection to storage. The re-electrification of stored hydrogen via fuel cells appears in cumulative terms, constrained by the annual hydrogen production and the efficiencies of the P2P components. The remaining electrical generation is also accounted for in cumulative terms, without attempting to define specific operating profile and capacity. Simply, a combination of dispatchable resources is assumed to always be available to meet the demand when solar and wind are not available (up to the maximum peak of residual load, which is in the range 30-38 GW).

Figure 10 presents the obtained combinations of solar PV and wind capacity together with required electrolysis size (through the color scale) for different imposed RES shares. The smallest wind capacity value considered is the current installation. The curve shape is similar for all the values of RES share: at growing wind capacity, the needed PV installation decreases. As noticed in Figure 3, the required electrolysis capacity varies with the wind/PV ratio and presents an intermediate minimum, which appears at lower wind installation when the desired RES share decreases. In other words, it is possible to minimize the required electrolysis capacity by targeting an appropriate mix of PV and wind. The range of electrolysis capacity is wide. Installations as low as 32 GW are compatible with an 80% RES scenario, whereas electrolyzer system capacities above 100 GW are required at low wind installed capacity when RES shares larger than 90% are imposed. At high installed capacity, wind power is able to meet a RES share up to 95% without any solar PV. However, such a high capacity level should be considered a stretch goal that is not as realistic as a mix of technologies.

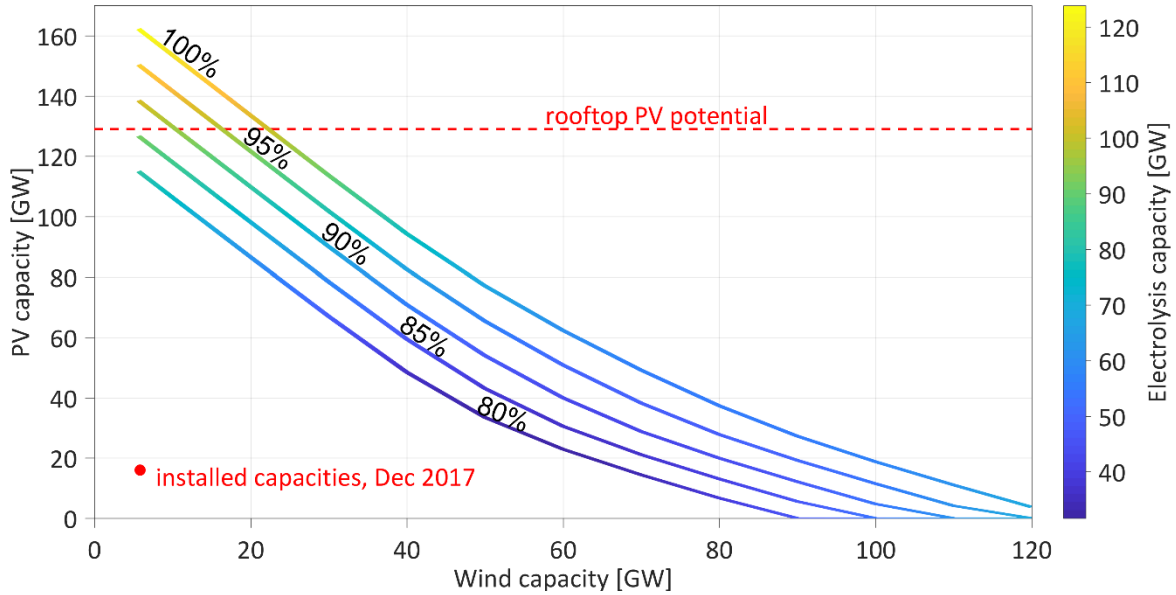

Figure 10 – Sets of combinations of capacities (PV, wind, and electrolysis systems) that guarantee a specified RES share.

Hydrogen storage capacity

All results presented so far assume that adequate capacity is available to hourly, daily, and seasonally store hydrogen. In this section, the hydrogen energy storage capacity is evaluated, discussed, and then compared to some existing natural gas delivery and storage infrastructure.

Figure 11 shows the annual profiles of stored hydrogen in 9 simulated cases. The stored amount at the end of the simulated period is equal to the quantity at the start, thus enabling a balanced hydrogen storage in subsequent periods and allowing a fair comparison. For each curve, the maximum corresponds to the needed storage capacity, which ranges from 770 kt to 1080 kt (equivalent to 25-36 TWh_{LHV}, based on LHV_{H2}). As a reference, 1000 kt of H_2 have the same energy content (33.3 TWh_{LHV}) as 3.6 billion Sm^3 of methane.

The required hydrogen storage capacity increases with the installed wind power capacity, due to the greater seasonal dependence of wind generation. On the contrary, capacity needs in high-solar cases benefit from the more predictable generation profile across seasons (see Figure 12). Generally speaking, the storage system is filled up during the months of more intense RES availability (left part of Figure 12), then emptied in the winter period and filled up again in spring. Also, a shift in time of the storage-filling period occurs when PV is the dominant technology, showing a later start of the discharge corresponding to a longer high-yield period of PV. While solar-dominated cases present daily fluctuations continuously along the year, high-wind cases feature some intermediate spikes related to the more irregular generation profile. In general, introduction of limitations on P2P capacities is beneficial because they shift down the storage profile by reducing the production, in spite of higher installed RES capacity and curtailment. This is consistent with the previous finding that some amount of RES power curtailment is likely desired to minimize cost.

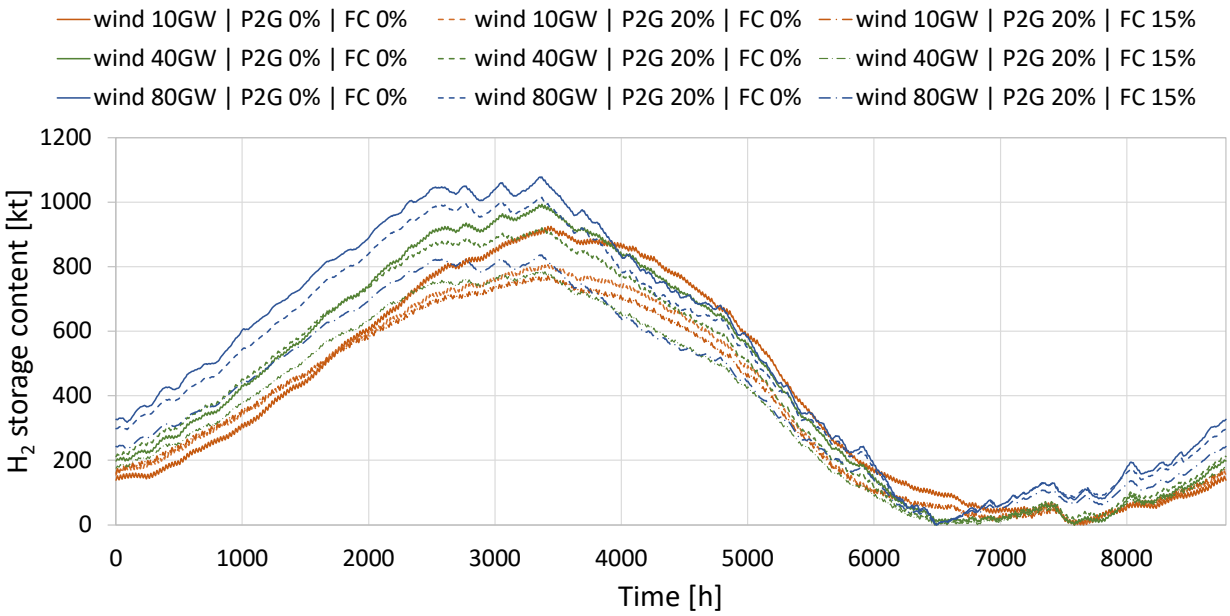

Figure 11 – Hydrogen storage profiles in 9 simulated cases, at 3 values of wind capacity; percentage values in the legend are the assigned minimum capacity factors for electrolyzers (P2G) and fuel cells (FC). Time axis starts on June 1st.

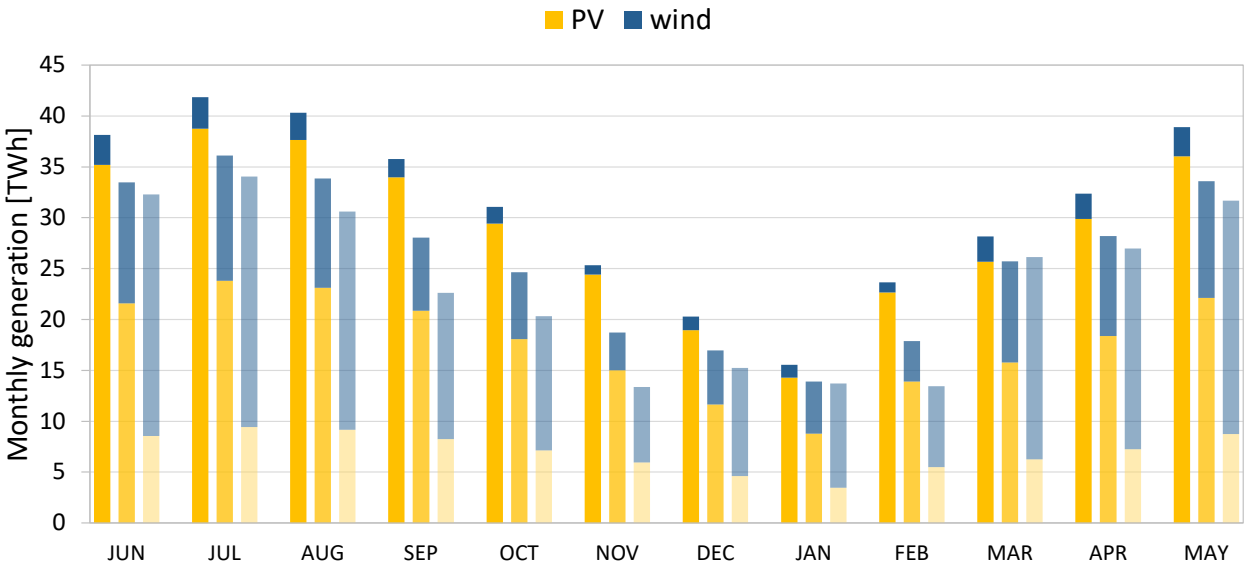

Figure 12 – Monthly generation by wind and solar in three simulated cases of assigned wind capacity of 10 GW, 40 GW, and 80 GW (in order of increased fading, respectively).

To assess the magnitude of the hydrogen storage capacity required in our analyses, the quantities may be compared to other energy storage solutions deployed in the same region. Table 4 lists the most relevant storage options available in California, detailing their capacity both as LHV energy content and as electric-equivalent energy[4]. Pumped hydro storage plants are a mature technology; but, with about 4 GW of power capacity [55] and less than 3 TWh_{el} of energy capacity, they can play only a limited role as alternative to new technologies like P2P and BESS (increase is unlikely due to lack of sites and difficult social acceptance). Existing natural gas storage facilities are mostly depleted oil and gas fields and have a working capacity of about 10 billion Sm^3 (total

[4] Fuel-to-electricity conversion efficiency is assumed equal to 64% in both cases, corresponding to the value used in the calculations for fuel cell systems and also demonstrated in the most recent developments for combined-cycle power plants [68].

storage capacity is 17 billion Sm^3). Further capacity may become available in future when currently operating wells will end production. Natural gas is also stored as linepack in the transmission and distribution grid, with the former capable to host as much as 4 TWh_{LHV} of natural gas when assuming to entirely fill it at 7.5 MPa. Table 4 includes also estimates of the potential for hydrogen storage in natural gas infrastructures. Indeed, various studies have given a positive answer when assessing the suitability of either a partial admixture [56] (e.g., up to 20%$_{vol}$ [57]) or a complete switch [58].

Other typical bulk hydrogen storage options include salt caverns [59] and lined rock caverns. There is no known availability of salt caverns in California [60]. Ongoing research is investigating lined rock caverns as a promising future technology that shows wider adaptability to different terrains [49,61].

Table 4 - List of storage capacities in California, as of currently used and in case of hydrogen introduction. Electric-equivalent values assume a fuel-to-electricity conversion efficiency of 64%.

	Unit	***Value***	***Ref.***
Pumped hydro storage plants	Electric-equivalent energy	2.59 TWh_{el}	[62]
Existing NG underground storage facilities	Working volume	10.52 billion Sm^3	[60]
	NG LHV energy	93.20 TWh_{LHV}	
	NG electric-equivalent energy	59.64 TWh_{el}	
	H2 LHV (100% substitution)	29.95 TWh_{LHV}	
	H2 electric-equivalent energy (100% substitution)	19.17 TWh_{el}	
Natural gas grid (linepack at 7.5 MPa)	NG LHV energy	4.04 TWh_{LHV}	[63]
	NG electric-equivalent energy	2.59 TWh_{el}	
	H2 LHV energy (20%$_{vol}$ admixing)	0.26 TWh_{LHV}	
	H2 electric-equivalent energy (20%$_{vol}$ admixing)	0.17 TWh_{el}	
	H2 LHV energy (100% substitution)	1.30 TWh_{LHV}	
	H2 electric-equivalent (100% substitution)	0.83 TWh_{el}	
Natural gas grid yearly transported amount	NG volume	61.66 billion Sm^3	[60]
	NG LHV energy	546.59 TWh_{LHV}	
	NG electric-equivalent energy	349.82 TWh_{el}	
	H2 LHV energy (at 20%$_{vol}$ mix)	35.11 TWh_{LHV}	
	H2 electric-equivalent energy (at 20%$_{vol}$ mix)	22.47 TWh_{el}	

Preliminary economic outlook

Although an economic analysis is beyond the scope of this work, it is interesting to roughly estimate the cumulative cost of the proposed storage systems. Table 5 presents the investment cost related to the sets of generation and storage capacities that could attain a 100% renewable electricity supply when 40 GW of wind capacity are installed, in the P2P-only and in the BESS-only cases. Future cost estimates vary significantly in different literature sources. Here, the assumed specific costs are taken from medium-term estimates with either a US or a global perspective. In particular, studies by IRENA investigated the expected global average investment cost for wind and solar PV plants [64] and the projected capital cost reduction for BESS [65]. A review of studies about investment cost for electrolysis systems narrows the range to 397-955 €/kW_{HHV} in the 2030 timeframe [66], and the mean value is considered for the calculations (after conversion to USD assuming 1.16 $/€ as the exchange rate). Stationary fuel cell systems and underground hydrogen storage have been investigated by Sandia National Laboratories [67]. The total investment cost for the storage system amounts to $73 billion when using hydrogen as storage means, or more than $4 trillion for BESS as the exclusive storage technology. For comparison, we note that the estimates for BESS reported by a recent study [27] is also on the

order of a few $ trillion. These types of results are expected due to the fundamental difference between battery energy storage and hydrogen energy storage systems, that is, power capacity (electrolyzer and fuel cell capacities) and energy capacity (hydrogen storage capacity) scale independently for hydrogen storage, whereas they are completely coupled for battery energy storage systems.

Table 5 – Estimation of investment costs for the generation and storage systems in the simulated scenario, at wind capacity equal to 40 GW (1 G$ = $1 billion).

	Specific cost	***Ref.***	***P2P***		***BESS***	
			Capacity	***Cost***	***Capacity***	***Cost***
Wind	1370 $/kW	[64]	40.0 GW	54.8 G$	40.0 GW	54.8 G$
Solar PV	790 $/kW	[64]	94.3 GW	74.5 G$	70.7 GW	55.9 G$
Total cost (RES power generation)	-	-	-	129.3 G$	-	110.7 G$
Electrolysis systems	600 $/kW$_{el}$	[66]	77.0 GW	46.4 G$	-	-
Fuel cell systems	500 $/kW$_{el}$	[67]	33.3 GW	16.7 G$	-	-
H2 storage (underground)	0.3 $/kWh	[67]	1022 kt	10.2 G$	-	-
BESS	150 $/kWh	[65]	-	-	27.0 TWh	4046.2 G$
Total cost (storage)	-	-	-	73.3 G$	-	4046.2 G$

Keeping in mind the preliminary scope of these economic considerations, it is possible to see how the P2P storage system based on hydrogen technology may be orders of magnitude less expensive than a BESS system. Even if one assumes a halving of the BESS cost and a doubling of the P2P cost, the hydrogen-based system would still show a 14x lower cost. In the proposed scenario, the complete P2P storage system would imply an investment cost which adds almost 60% of the wind+PV RES power generation system costs required to reach the ambitious 100% RES scenario. With the cost trends associated with wind and solar power generation that predict 30-60 $/MWh as levelized cost of electricity [64], such an economic impact should be considered reasonable and achievable (leading to levelized costs of electricity in the range of 47-94 $/MWh).

Summary and conclusions

A model has been developed to simulate the energy balance within a large-scale regional electric system, under the assumption of a single-node power grid. It focuses on the calculation of residual load after renewable energy sources are deployed, and integrates hydrogen storage into the system, based on the use of electrolyzers, fuel cells, and hydrogen storing facilities. The aim is to assess the requirements to maintain grid operations (balance load with generation) while achieving complete coverage of electric load by means of only wind and solar resources. The model scales combinations of historically measured solar and wind power dynamics to very large installed capacities.

Simulations of the California power system show that reaching 100% renewable electricity supply is technically feasible within the available RES resource potential in the state. However, wind and solar installation needs to grow very significantly from current capacities, and significant electric energy storage capacity is needed. Assuming we can exploit Power-to-Power systems to produce hydrogen during overgeneration and reconvert it to electricity when needed, the complete elimination of fossil fuels from the power system would require high-PV combinations like 94 GW PV + 40 GW wind or a high-wind mix such as 37 GW PV + 80 GW wind, to be coupled with hydrogen energy storage as large as 77 GW of electrolysis capacity and 33 GW of fuel cell capacity in the first case, or 55 GW of electrolysis capacity and 30 GW fuel cell capacity in the second case. Real operation of electrolyzers and fuel cells is likely to limit the installed capacity in order to guarantee a high capacity factor. Sensitivity analyses on the imposed actual full-load hours (i.e., minimum CF on an hourly basis) show that

limited and somewhat beneficial variations occur. In the alternative case of BESS as the only storage technology, their higher efficiencies allow the power system to meet 100% renewable electricity supply with lower RES installed capacities, while requiring to complement them with around 30 TWh of BESS energy capacity.

A reduction of the required share of wind and solar from 100% to 90% would reduce the installed PV capacity by 15-25% in the low-wind cases (10-40 GW wind capacity) or by up to 75% in the high-wind case (120 GW wind capacity). The corresponding electrolysis system capacity reduction is in the order of 18-27%, while total fuel cell system capacity depends rather upon specific dispatch choices. To guarantee clean electricity supply, this requires the identification of complementary energy storage and dispatchable power generation technologies, e.g., dispatchable renewable power systems such as those that operate on biomass or biofuels.

Furthermore, a preliminary economic analysis shows the potential attractiveness of the hydrogen-based P2P storage system compared to a BESS-based system. It also indicates that the overall capital cost of the proposed P2P storage system is equal to about 60% of the investment cost of the required RES power generation infrastructure. In contrast, an alternative purely electric BESS-based storage system would increase costs massively.

Long-term evolution of the energy system will involve stronger interactions among sectors, like residential heating, industrial fuel demand, and transportation. A foreseen development of the study aims at analyzing the effects of electrical load and hydrogen demand variations from the introduction of innovative transportation modes like plug-in electric vehicles and hydrogen fuel cell vehicles.

Acknowledgements

The authors gratefully acknowledge the Ministry of Education, Universities, and Research (Italy) and the Southern California Gas Company (USA) for partial financial support of this work, as well as Edison SpA (Italy) for the fruitful discussions on P2G development.

Nomenclature and acronyms

AFLH	Actual Full-Load Hours [h/y]	IRENA	International Renewable Energy Agency
BESS	Battery Energy Storage System	ISO	Independent System Operator
CAISO	California Independent System Operator	LHV	Lower Heating Value
CF	Capacity Factor [%]	NG	Natural Gas
CSP	Concentrated Solar Power	PEM	Proton Exchange Membrane
EFLH	Equivalent Full-Load Hours [h/y]	PV	Photovoltaic
EOC	Equivalent Operating Cycles [cycles/y]	P2G	Power-to-Gas
EOH	Equivalent Operating Hours [h/y]	P2G2P	Power-to-Gas-to-Power
FC	Fuel Cell	P2P	Power-to-Power
GHG	Greenhouse Gas	RES	Renewable Energy Sources
HHV	Higher Heating Value	RL	Residual Load
H2	Hydrogen		

References

[1] IPCC 2014, Climate Change 2014: Synthesis Report. Contribution of Working Groups I, II and III to the Fifth Assessment Report of the Intergovernmental Panel on Climate Change, IPCC, Geneva, Switzerland, 2014.

[2] European Commission, Communication from the Commission to the European Parliament, the Council, the European Economic and Social Committee and the Committee of the Regions. A roadmap for moving to a competitive low carbon economy in 2050, 2011.

[3] G. Strbac, Demand side management: Benefits and challenges, Energy Policy. 36 (2008) 4419–4426. doi:10.1016/j.enpol.2008.09.030.

[4] California ISO, Reliability requirements. http://www.caiso.com/planning/Pages/ReliabilityRequirements/Default.aspx (accessed April 10, 2018).

[5] California Senate Bill No. 100. An act to amend Sections 399.11, 399.15, and 399.30 of, and to add Section 454.53 to, the Public Utilities Code, relating to energy., 2017.

[6] California State Assembly Bill No. 32. An act to add Division 25.5 (commencing with Section 38500) to the Health and Safety Code, relating to air pollution., 2006.

[7] California Senate Bill No. 1275. An act to amend Section 44125 of, and to add Chapter 8.5 (commencing with Section 44258) to Part 5 of Division 26 of, the Health and Safety, relating to vehicular air pollution., 2014.

[8] European Commission, Communication from the Commission to the European Parliament, the Council, the European Economic and Social Committee and the Committee of the Regions. A policy framework for climate and energy in the period from 2020 to 2030, 2014.

[9] IEA (International Energy Agency), Technology Roadmap - Solar Photovoltaic Energy, 2014.

[10] Bloomberg New Energy Finance, New Energy Outlook 2018, 2018.

[11] PricewaterhouseCoopers (PwC), Potsdam Institute for Climate Impact Research (PIK), International Institute for Applied Systems Analysis (IIASA), European Climate Forum (ECF), 100% renewable electricity. A roadmap to 2050 for Europe and North Africa, 2010.

[12] A. Blakers, B. Lu, M. Stocks, 100% renewable electricity in Australia, Energy. 133 (2017) 471–482. doi:10.1016/j.energy.2017.05.168.

[13] M.R. Shaner, S.J. Davis, N.S. Lewis, K. Caldeira, G[1] M.R. Shaner, S.J. Davis, N.S. Lewis, K. Caldeira, Geophysical constraints on the reliability of solar and wind power in the United States, Energy & Environmental Science. 11 (2018) 914–925. doi:10.1039/C7EE03029K.eophysical constraints on the reliabi, Energy & Environmental Science. 11 (2018) 914–925. doi:10.1039/C7EE03029K.

[14] A. Gulagi, D. Bogdanov, C. Breyer, The Demand for Storage Technologies in Energy Transition Pathways Towards 100% Renewable Energy for India, Energy Procedia. 135 (2017) 37–50. doi:10.1016/j.egypro.2017.09.485.

[15] N. Ghorbani, A. Aghahosseini, C. Breyer, Transition towards a 100% Renewable Energy System and the Role of Storage Technologies: A Case Study of Iran, Energy Procedia. 135 (2017) 23–36. doi:10.1016/j.egypro.2017.09.484.

[16] A. Sadiqa, A. Gulagi, C. Breyer, Energy transition roadmap towards 100% renewable energy and role of storage technologies for Pakistan by 2050, Energy. 147 (2018) 518–533. doi:10.1016/j.energy.2018.01.027.

[17] U. Caldera, D. Bogdanov, S. Afanasyeva, C. Breyer, Integration of reverse osmosis seawater desalination in the power sector, based on PV and wind energy, for the Kingdom of Saudi Arabia, in: 32nd European Photovoltaic Solar Energy Conference, 2016.

[18] M.Z. Jacobson, M.A. Delucchi, Z.A.F. Bauer, S.C. Goodman, W.E. Chapman, M.A. Cameron, C. Bozonnat, L. Chobadi, H.A. Clonts, P. Enevoldsen, J.R. Erwin, S.N. Fobi, O.K. Goldstrom, E.M. Hennessy, J. Liu, J. Lo, C.B. Meyer, S.B. Morris, K.R. Moy, P.L. O'Neill, I. Petkov, S. Redfern, R. Schucker, M.A. Sontag, J. Wang, E. Weiner, A.S. Yachanin, 100% Clean and Renewable Wind, Water, and Sunlight All-Sector Energy Roadmaps for 139 Countries of the World, Joule. 1 (2017) 108–121. doi:10.1016/j.joule.2017.07.005.

[19] European Renewable Energy Council, Re-thinking 2050. A 100% Renewable Energy Vision for the European Union, 2010.

[20] California ISO, Managing oversupply. http://www.caiso.com/informed/Pages/ManagingOversupply.aspx (accessed January 16, 2018).

[21] IRENA, Battery storage for renewables: market status and technology outlook, 2015.

[22] M. Lehner, R. Tichler, H. Steinmueller, M. Koppe, Power-to-Gas: Technology and Business Models, Springer, 2014.

[23] M. Ludwig, C. Haberstroh, U. Hesse, Exergy and cost analyses of hydrogen-based energy storage pathways for residual load management, International Journal of Hydrogen Energy. 40 (2015) 11348–11355. doi:10.1016/j.ijhydene.2015.03.018.

[24] Itron, 2014-2015 SGIP Impacts Evaluation, 2016. http://www.cpuc.ca.gov/General.aspx?id=7890.

[25] Terna, Report di esercizio I anno di sperimentazione - Sperimentazione di progetti pilota di accumulo energetico a batterie di tipo energy intensive, 2017. http://download.terna.it/terna/0000/0934/81.PDF.

[26] H. Ameli, M. Qadrdan, G. Strbac, Techno-economic assessment of battery storage and Power-to-Gas: A whole-system approach, Energy Procedia. 142 (2017) 841–848. doi:10.1016/j.egypro.2017.12.135.

[27] J. Temple, The $2.5 trillion reason we can't rely on batteries to clean up the grid, (2018). https://www.technologyreview.com/s/611683/the-25-trillion-reason-we-cant-rely-on-batteries-to-clean-up-the-grid/.

[28] P. Hollmuller, J.-M. Joubert, B. Lachal, K. Yvon, Evaluation of a 5 kWp photovoltaic hydrogen production and storage installation

for a residential home in Switzerland, International Journal of Hydrogen Energy. 25 (2000) 97–109. doi:10.1016/S0360-3199(99)00015-4.

[29] J.D. Maclay, J. Brouwer, G.S. Samuelsen, Dynamic modeling of hybrid energy storage systems coupled to photovoltaic generation in residential applications, Journal of Power Sources. 163 (2007) 916–925. doi:10.1016/j.jpowsour.2006.09.086.

[30] J.D. Maclay, J. Brouwer, G. Scott Samuelsen, Dynamic analyses of regenerative fuel cell power for potential use in renewable residential applications, International Journal of Hydrogen Energy. 31 (2006) 994–1009. doi:10.1016/j.ijhydene.2005.10.008.

[31] Grasshopper Project - Grid Assisting Modular Hydrogen PEM Power Plant. http://www.grasshopperproject.eu/.

[32] B. Nastasi, G. Lo Basso, D. Astiaso Garcia, F. Cumo, L. de Santoli, Power-to-gas leverage effect on power-to-heat application for urban renewable thermal energy systems, International Journal of Hydrogen Energy. (2018). doi:10.1016/J.IJHYDENE.2018.08.119.

[33] M. Bailera, P. Lisbona, Energy storage in Spain: forecasting electricity excess and assessment of Power-to-Gas potential up to 2050, Energy. 143 (2018) 900–910. doi:10.1016/j.energy.2017.11.069.

[34] G. Guandalini, M. Robinius, T. Grube, S. Campanari, D. Stolten, Long-term power-to-gas potential from wind and solar power: A country analysis for Italy, International Journal of Hydrogen Energy. 42 (2017) 1–18. doi:10.1016/j.ijhydene.2017.03.081.

[35] P. Colbertaldo, G. Guandalini, S. Campanari, Modelling the integrated power and transport energy system: The role of power-to-gas and hydrogen in long-term scenarios for Italy, Energy. 154 (2018) 592–601. doi:10.1016/j.energy.2018.04.089.

[36] C.J. Greiner, M. Korpås, A.T. Holen, A Norwegian case study on the production of hydrogen from wind power, International Journal of Hydrogen Energy. 32 (2007) 1500–1507. doi:10.1016/j.ijhydene.2006.10.030.

[37] S. Mesfun, D.L. Sanchez, S. Leduc, E. Wetterlund, J. Lundgren, M. Biberacher, F. Kraxner, Power-to-gas and power-to-liquid for managing renewable electricity intermittency in the Alpine Region, Renewable Energy. 107 (2017) 361–372. doi:10.1016/j.renene.2017.02.020.

[38] E. Haghi, M. Fowler, K. Raahemifar, Co-benefit analysis of incentives for energy generation and storage systems: a multi-stakeholder perspective, International Journal of Hydrogen Energy. (2018). doi:10.1016/j.ijhydene.2018.08.150.

[39] U.S. Energy Information Administration (US-EIA), Assumptions to the Annual Energy Outlook 2018. Electricity Market Module, Washington, DC, USA, 2018. https://www.eia.gov/outlooks/aeo/assumptions/.

[40] J. Tomei, Planning for a Transition to a Hydrogen Economy: A Review of Roadmaps, London, UK, 2009.

[41] A. Van Stiphout, K. De Vos, G. Deconinck, Operational flexibility provided by storage in generation expansion planning with high shares of renewables, in: 12th International Conference on the European Energy Market, EEM, 2015. doi:10.1109/EEM.2015.7216760.

[42] California Energy Commission, Tracking Progress. Renewable Energy, 2017.

[43] U.S. Energy Information Administration (US-EIA), Electric Power Monthly, n.d. https://www.eia.gov/electricity/monthly/.

[44] NREL (National Renewable Energy Laboratory), Geospatial Data Science - Data Visualization and Geospatial Tools. https://www.nrel.gov/gis/tools.html (accessed November 16, 2017).

[45] A. Lopez, B. Roberts, D. Heimiller, N. Blair, G. Porro, U.S. Renewable Energy Technical Potentials: A GIS-Based Analysis, Golden, CO, US, 2012.

[46] P. Gagnon, R. Margolis, J. Melius, C. Phillips, R. Elmore, Rooftop Solar Photovoltaic Technical Potential in the United States: A Detailed Assessment, Golden, CO, US, 2016.

[47] California Energy Commission, Tracking Progress. California's Installed Electric Power Capacity and Generation, 2017.

[48] Fuel Cells and Hydrogen Joint Undertaking, Development of Water Electrolysis in the European Union, 2014.

[49] B. Žlender, S. Kravanja, Cost optimization of the underground gas storage, Engineering Structures. 33 (2011) 2554–2562. doi:10.1016/j.engstruct.2011.05.001.

[50] IEA Greenhouse Gas R&D Programme (IEA GHG), Co-Production of Hydrogen and Electricity by Coal Gasification with CO2 Capture - Updated Economic Analysis (Attachment C: Hydrogen Storage), 2008. https://ieaghg.org/docs/General_Docs/Reports/2008-9.pdf.

[51] Fuel Cell & Hydrogen Energy Association (FCHEA), Commercially Available Fuel Cell & Related Products, 2017. http://www.fchea.org/reports/.

[52] P. Kurzweil, Lithium Battery Energy Storage: State of the Art Including Lithium-Air and Lithium-Sulfur Systems, in: P.T. Moseley, J. Garche (Eds.), Electrochemical Energy Storage for Renewable Sources and Grid Balancing, Elsevier B.V., 2014: pp. 269–307. doi:10.1016/B978-0-444-62616-5.00016-4.

[53] D. Stolten, B. Emonts, T. Grube, M. Weber, Hydrogen as an Enabler for Renewable Energies, in: D. Stolten, V. Scherer (Eds.), Transition to Renewable Energy Systems, Wiley-VCH Verlag GmbH & Co. KGaA, Weinh, 2013: pp. 195–215. doi:10.1002/9783527673872.ch12.

[54] M. Kopp, D. Coleman, C. Stiller, K. Scheffer, J. Aichinger, B. Scheppat, Energiepark Mainz: Technical and economic analysis of the worldwide largest Power-to-Gas plant with PEM electrolysis, International Journal of Hydrogen Energy. 42 (2017) 13311–13320. doi:10.1016/j.ijhydene.2016.12.145.

[55] US-DOE Office of Electricity Delivery & Energy Reliability, Global Energy Storage Database. http://www.energystorageexchange.org/ (accessed December 15, 2018).

[56] M.W. Melaina, O. Antonia, M. Penev, Blending Hydrogen into Natural Gas Pipeline Networks: A Review of Key Issues, 2013. doi:10.2172/1068610.

[57] K. Altfeld, D. Pinchbeck, Admissible hydrogen concentrations in natural gas systems, Gas for Energy. (2013) 1–16. doi:ISSN 2192-158X.

[58] D. Sadler, A. Cargill, M. Crowther, A. Rennie, J. Watt, S. Burton, M. Haines, H21 Leeds City Gate Report, 2016. https://www.northerngasnetworks.co.uk/wp-content/uploads/2017/04/H21-Report-Interactive-PDF-July-2016.compressed.pdf.

[59] H. Blanco, A. Faaij, A review at the role of storage in energy systems with a focus on Power to Gas and long-term storage, Renewable and Sustainable Energy Reviews. 81 (2018) 1049–1086. doi:10.1016/j.rser.2017.07.062.

[60] U.S. Energy Information Administration (US-EIA), Natural Gas Data. https://www.eia.gov/naturalgas/data.php (accessed July 19, 2018).

[61] Sofregaz US Inc., LRC, Commercial potential of natural gas storage in Lined Rock Caverns (LRC). Topical report prepared for U.S. Department of Energy, 1999. https://www.netl.doe.gov/File Library/Research/Oil-Gas/Natural Gas/other/34348_final.pdf.

[62] California Natural Resources Agency, Open Data - Water. https://data.cnra.ca.gov/group/water (accessed June 19, 2018).

[63] California Energy Commission, GIS Open Data. https://cecgis-caenergy.opendata.arcgis.com/ (accessed January 16, 2018).

[64] IRENA, The Power to Change: Solar and Wind Cost Reduction Potential to 2025, 2016. http://www.irena.org/-/media/Files/IRENA/Agency/Publication/2016/IRENA_Power_to_Change_2016.pdf.

[65] IRENA, Electricity Storage and Renewables: Costs and Market to 2030, Abu Dhabi, 2017. http://www.irena.org/-/media/Files/IRENA/Agency/Publication/2017/Oct/IRENA_Electricity_Storage_Costs_2017.pdf.

[66] S.M. Saba, M. Müller, M. Robinius, D. Stolten, The investment costs of electrolysis - A comparison of cost studies from the past 30 years, International Journal of Hydrogen Energy. 43 (2018) 1209–1223. doi:10.1016/j.ijhydene.2017.11.115.

[67] S. Schoenung, Economic Analysis of Large-Scale Hydrogen Storage for Renewable Utility Applications, Albuquerque, NM, USA and Livermore, CA, USA, 2011. http://prod.sandia.gov/techlib/access-control.cgi/2011/114845.pdf.

[68] A. Larson, Gas Power Generation Thrives, Turbine Manufacturers Struggle, Power Magazine. (2018). https://www.powermag.com/gas-power-generation-thrives-turbine-manufacturers-struggle/?pagenum=2.